Heterogenized C-Scorpionate Iron(II) complex on nanostructured carbon materials as recyclable catalysts for microwave-assisted oxidation reactions

Ribeiro, Ana P.C.; Martins, Luísa M.D.R.S.; Carabineiro, Sónia A.C.; Buijnsters, Josephus G.; Figueiredo, José L.; Pombeiro, Armando J.L.

DOI
10.1002/cctc.201702031

Publication date
2018

Document Version
Final published version

Published in
ChemCatChem

ChemPubSoc Europe

DOI: 10.1002/cctc.201702031

CHEMCATCHEM Full Papers

Heterogenized C-Scorpionate Iron(II) Complex on Nanostructured Carbon Materials as Recyclable Catalysts for Microwave-Assisted Oxidation Reactions

Ana P. C. Ribeiro,[a] Luísa M. D. R. S. Martins,*[a] Sónia A. C. Carabineiro,*[b] Josephus G. Buijnsters,[c] José L. Figueiredo,[b] and Armando J. L. Pombeiro[a]

The C-scorpionate iron(II) complex [$FeCl_2$(Tpm)] [Tpm = κ^3-$HC(C_3H_3N_2)_3$] (**1**) was immobilized on five different nanostructured carbon materials (nanodiamonds, graphene nanoplatelets, graphene oxide, reduced graphene oxide, and nanohorns) to produce active, selective, and recyclable catalysts for alkane and alcohol oxidations. The heterogenized systems (including the first ever reported complexes supported on carbon nanohorns) exhibited good activity concomitant with rather high selectivity to the formation of ketone alcohol (KA) oil (cyclohexanol and cyclohexanone mixture, yields up to 29%) from microwave-assisted oxidation of cyclohexane, and allowed their easy recovery and reuse, at least for five consecutive cycles maintaining 90.3% of the initial activity. Moreover, the functionalized nanodiamond supports (used for the first time as supports for iron complexes) were also able to effectively (yields up to 97%) catalyze the microwave-induced oxidation of 1- and 2-phenylethanol to acetophenone and 2-phenylacetaldehyde, respectively, and could be reused for seven consecutive cycles without losing catalytic activity.

Introduction

Currently, industrial catalytic oxidations are one of the most important processes to produce useful value-added chemical compounds from petroleum-based materials.[1] However, several are energy-intensive low efficiency processes and the search for efficient, selective, environmentally benign, and economic catalytic oxidation methods towards the sustainable development of chemical processes is urgent.

Many of the green benefits of homogeneous catalytic systems arise from designed catalysts based on transition metals with appropriate ligands. Tris(pyrazol-1-yl)methane transition-metal complexes have already been successfully applied as homogeneous catalysts for relevant industrial oxidation reactions, namely the challenging selective oxidations of alkanes to alcohols and ketones[2] or to carboxylic acids.[3]

The immobilization of a molecular catalyst in an inert support can improve its catalytic activity and allow its easier separation and recycling, which are required conditions in sustainable processes. Therefore, the combination of the properties of homogeneous complexes with the advantages of heterogeneous systems is obtained.

One of the approaches is to use porous materials based on carbon, which show a high surface area and can be bonded to a metallic complex, increasing its catalytic activity, compared with the bulk counterparts.

As iron is readily available, has low price, and low toxicity, Fe complexes have been widely used in homogeneous catalysis.[3,4] In particular, the C-scorpionate iron(II) complex [$FeCl_2$(Tpm)] [Tpm = κ^3-$HC(C_3H_3N_2)_3$, (**1**), Figure 1] is of particular interest, as previous works by us showed it to be quite active, either homogeneously or heterogenized in several materials, for a number of reactions, including the oxidation of alcohols and alkanes.[3,4c,k,q,r,x,aa–ac]

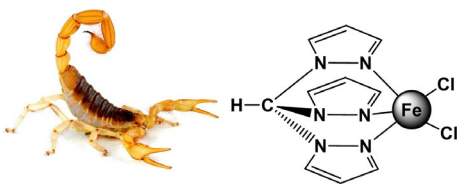

Figure 1. Hydrotris(pyrazol-1-yl)methane iron(II) complex **1**. The ligand is designated as scorpionate as it is able to bind to the metal like a scorpion attack, with the two claws and the tail.

[a] *Dr. A. P. C. Ribeiro, Prof. L. M. D. R. S. Martins, Prof. A. J. L. Pombeiro*
Centro de Química Estrutural
Instituto Superior Técnico, Universidade de Lisboa
Av. Rovisco Pais 1049-001 Lisboa (Portugal)
E-mail: luisamargaridamartins@tecnico.ulisboa.pt

[b] *Dr. S. A. C. Carabineiro, Prof. J. L. Figueiredo*
Laboratório de Catálise e Materiais
Laboratório Associado LSRE-LCM
Faculdade de Engenharia, Universidade do Porto
Rua Dr. Roberto Frias 4200-465 Porto (Portugal)
E-mail: sonia.carabineiro@fe.up.pt

[c] *Dr. J. G. Buijnsters*
Department of Precision and Microsystems Engineering
Research Group of Micro and Nano Engineering
Delft University of Technology
Mekelweg 2, 2628 CD Delft (The Netherlands)

Supporting information and the ORCID identification number(s) for the author(s) of this article can be found under https://doi.org/10.1002/cctc.201702031.

This manuscript is part of a Special Issue on "Supported Molecular Catalysts".

There are some reports of heterogenization studies of iron complexes on carbon nanotubes,[5] including our own work with the above complex.[4q,x] However, there are only a few studies of heterogenization of Fe complexes on graphene derivatives,[6] and no literature involving nanodiamonds or carbon nanohorns. Moreover, the number of reports on heterogenization of any kind of metal complex on nanodiamonds is very limited,[7] and to the best of our knowledge, no complexes were previously anchored on carbon nanohorns.

In this work, several nanostructured carbon materials (nanodiamonds, graphene nanoplatelets, graphene oxide, reduced graphene oxide, and nanohorns) were used as supports for heterogenization of the C-scorpionate iron(II) complex [$FeCl_2$(Tpm)] (**1**). The carbon supports are illustrated in Figure 2. The graphene nanoplatelets (G-NPL) are few-layer graphene sheets with less than 15 nm thickness and 5 μm diameter. The graphene oxide (GO), an oxidized form of graphene with various oxygen-containing functionalities such as epoxide, carboxyl, and hydroxy groups, had a purity of 99% and a diameter of 1–5 μm and a thickness between 0.8 and 1.2 nm. The reduced graphene oxide (rGO) material was obtained by thermal shock reduction and had a purity of >99%, thickness of 1–2 layers, and a dimension of 1–5 μm. The single-walled carbon nanohorns (SWCNH) consist of tiny graphene sheets, wrapped to form horn-shaped cones with a half fullerene cap (similar to Dahlia flowers), with 30–50 nm length and 3–5 nm diameter. Nanodiamonds (ND) are nano-sized diamond particulates originated from a detonation process. As a result, they exhibit a narrow particle size distribution and a small particle size (< 10 nm) and are characterized by a sp^3-C core with a highly developed chemically active sp^2-C rich surface.

The obtained hybrid materials were used in microwave-assisted oxidation reactions, namely the oxidation of cyclohexane (Scheme 1) and of 1- and 2-phenylethanol (Scheme 2), which are reactions of industrial importance for the synthesis of commodities and fine chemicals.[1] The oxidation of cyclohexane produces selectively cyclohexanol and cyclohexanone, important reagents for the production of adipic acid and caprolactam used, for example, for the manufacture of nylon. Acetophenone and 2-phenylacetaldehyde, which are precursors to organic compounds ranging from pharmaceuticals to plastic additives,[9] were obtained by the catalytic oxidation of the corresponding alcohols.

The use of microwave (MW) irradiation in the above catalytic conversions was found to be advantageous, namely, leading to more efficient and faster processes operating at lower temperatures.[4v,x,z,9,10]

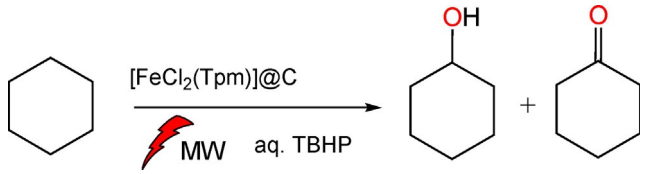

Scheme 1. MW-assisted oxidation of cyclohexane with aqueous *tert*-butyl hydroperoxide catalyzed by [$FeCl_2$(Tpm)] supported on different nanostructured carbon materials.

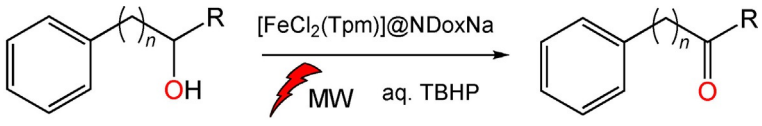

n = 0, R = Me; *n* = 1, R = H

Scheme 2. MW-assisted oxidation of 1- and 2-phenylethanol with aqueous *tert*-butyl hydroperoxide catalyzed by [$FeCl_2$(Tpm)] supported on functionalized nanodiamonds (NDoxNa).

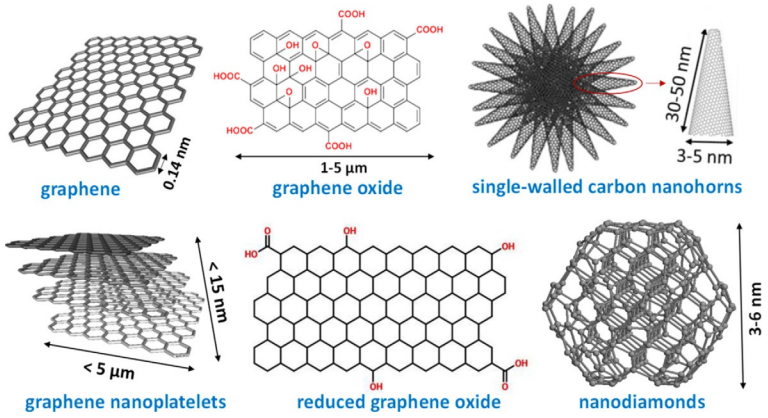

Figure 2. Carbon materials used as supports. Different structures, chemical treatments, geometries, and dimensions are presented. Structures are not to scale. The graphene structures are simplified models used for better comparison and comprehension; for a more realistic view, see, for example, Ref. [8].

Results and Discussion

Characterization of carbon supports

The carbon supports showed Brunauer–Emmett–Teller (BET) surface areas varying from 35 $m^2 g^{-1}$ (G-NPL) up to 450 $m^2 g^{-1}$ (for both GO and rGO). ND and SWCNH showed intermediate values of 295 and 304 $m^2 g^{-1}$, respectively. These values are in agreement with those reported by the suppliers.

The carbon supports were also analyzed by X-ray photoelectron spectroscopy (XPS). The obtained results are shown in Figure 3. The C 1s spectrum of SWCNH shows only three peaks (Figure 3a) that are attributed to sp^2 carbon, C-OH, and COOH.[11] The spectrum of G-NPL (Figure 3a) can be deconvoluted into four different peaks, attributed to sp^2 C=C (284.2 eV), C–OH (284.9 eV), C=O (286.9 eV), and COOH (291.3 eV).[12] The sp^2 peak of this material is much more intense than the analogue peaks of the other graphene derivative samples. The other peaks (C–OH, C=O, and COOH) have decreased intensities compared with the other materials. This shows that the amount of C=C bonds is higher in non-oxidized

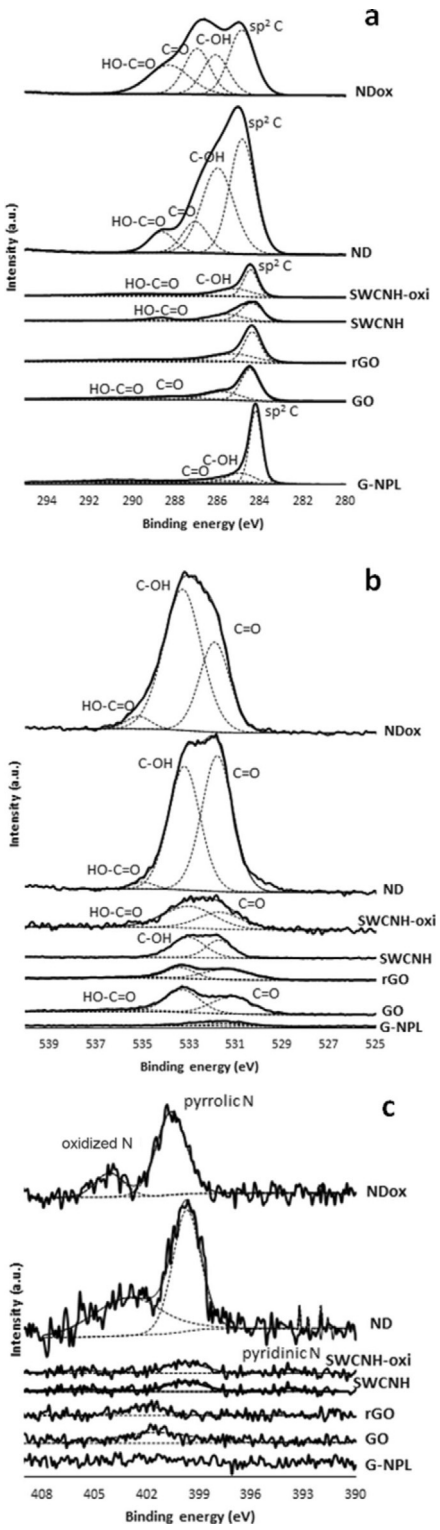

Figure 3. XPS of carbon supports: C 1s (a), O 1s (b), and N 1s (c).

graphene (G-NPL). Not surprisingly, GO and rGO have a higher number of oxygenated groups (a scheme of such groups is seen in Figure 4). ND and NDox also display four peaks, those of ND being more intense. However, the peak of HO-C=O (carboxylic acids) is larger for NDox, as expected, owing to the oxidation treatment.

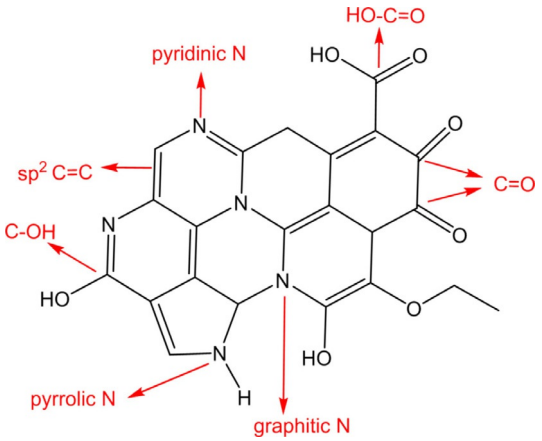

Figure 4. Schematic diagram of carbon, oxygen, and nitrogen moieties found on graphene.

The O 1s spectra are shown in Figure 3 b. The graphene-derived samples (G-NPL, GO, and rGO) show relatively weak signals attributed to C=O at lower binding energy values and others at slightly higher binding energies attributed to C–OH.[12c] The oxidized GO and rGO materials also show a small band at higher binding energy, attributed to COOH.[12c] The peaks obtained from the NDs are more intense than those of the other materials. Interestingly, the oxidized ND sample (NDox) displays more HO–C=O groups and less C=O moieties than ND.

The N 1s spectra (Figure 3 c) show very low intensity and are mostly noisy. SWCNH shows three types of N surface groups: oxidized (405.8 eV), pyrrolic (399.8 eV), and pyridinic (393.7 eV), shown in Figure 4.[12d] GO and rGO show peaks centered around 402 eV, which can be attributed to graphitic N. G-NPL shows no peaks related to nitrogen (only C and O), which is evidence for their high purity. Nevertheless, it is possible that very small amounts of graphitic and pyrrolic N do exist. Again, the spectra of ND and NDox are more intense that than those of the other samples. Larger amounts of pyrrolic and graphitic N are detected for both samples but, comparatively, no clear signals from pyridinic N are identified (Figure 3 c).

The morphology of the carbon materials was also examined by SEM (Figure S1 in the Supporting Information). Graphene materials show flakes with larger average sizes. The graphene sheets are well visible. There is a wide range of agglomerate sizes and overall shapes for the NDs and SWCNHs materials.

Heterogenization efficiency

The Fe complex was heterogenized on the different carbon materials (≈approx. 2% Fe w/w was the intended value, but different loadings were obtained as shown in Table 1).

All supports were able to anchor the Fe^{II} complex, although with different efficiencies (Table 1). It can be seen that **1** was heterogenized better on the oxidized surfaces (NDox, GO, and SWCNH-oxi). It is well known that the oxidation treatments increase the number of surface groups on the materials,[4q,x,7b,13] providing additional sites (see also Figure 3 b) for anchorage of

Table 1. Iron loadings obtained after heterogenization of the iron complex **1** on the different carbon materials.

Sample (**1**@carbon)	%Fe (w/w)
1@ND	1.13
1@NDox	1.57
1@NDoxNa	1.39
1@G-NPL	0.93
1@GO	1.54
1@rGO	0.88
1@SWCNH	1.67
1@SWCNH-oxi	1.90

the complexes. The morphology of the carbon materials with the anchored complex was also examined by SEM (Figure 5). The appearance of these materials is not very different from that of the supports (Figure S1 in the Supporting Information). The larger amplifications shown in Figure 5 allow us to better see the graphene sheets and also the protuberances of the SWCNH materials, with sizes similar to those depicted in Figure 2.

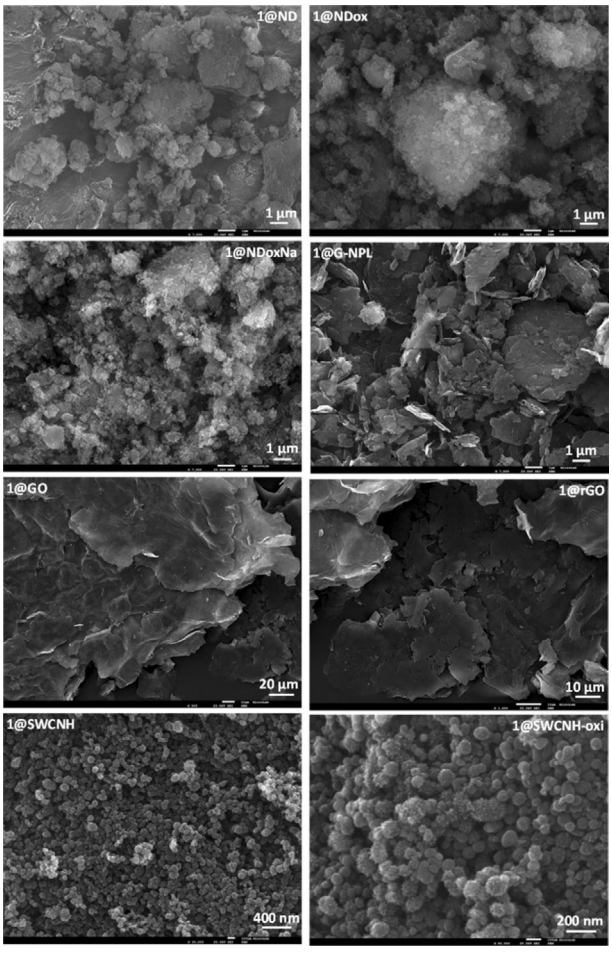

Figure 5. SEM images of the scorpionate complex [$FeCl_2$(Tpm)] [Tpm = κ^3-$HC(C_3H_3N_2)_3$] (**1**) supported on the different nanostructured carbon materials.

Microwave-assisted oxidation of cyclohexane

The catalytic systems for the oxidation of cyclohexane (Scheme 1) are based on the scorpionate complex [$FeCl_2$(Tpm)] [Tpm = κ^3-$HC(C_3H_3N_2)_3$] (**1**) supported on the nanostructured carbon materials (nanodiamonds, graphene nanoplatelets, graphene oxide, reduced graphene oxide, and nanohorns), the oxidant was *tert*-butyl hydroperoxide (TBHP, 70% aq. solution) and the solvent acetonitrile (MeCN) in acidic medium (pyrazine carboxylic acid, Hpca) and under microwave (MW) irradiation at 50 °C.

Under the optimized conditions (1.5 h irradiation), cyclohexanol (A) and cyclohexanone (K) were the only products detected by GC-MS analysis, indicating high selectivity of the tested oxidation systems. After 1.5 h of MW irradiation under the above conditions, the yield enhancement is not considerable (Figure 6 for **1**@SWCNH-oxi). Moreover, for longer reaction

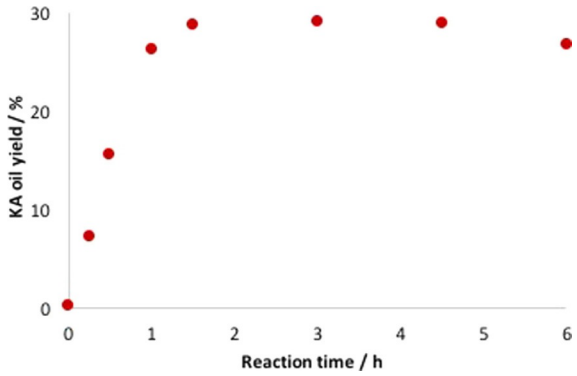

Figure 6. Effect of the reaction time on the yield of KA oil obtained from oxidation of cyclohexane catalyzed by **1**@SWCNH-oxi.

times (> 3 h), GC-MS analyses revealed the presence of 1,4-cyclohexanediol and 1,4-hydroxycyclohexanone. The formation of these side products of cyclohexane oxidation is believed to be the cause of the KA oil yield decrease observed for reaction times higher than 3 h as depicted in Figure 6 for **1**@SWCNH-oxi.

Control experiments in the absence of complex [$FeCl_2$(Tpm)] (**1**), with *t*BuOOH (Table 2, entry 10) confirm the crucial role of **1** to efficiently catalyze the oxidation of cyclohexane. The different bare carbon nanomaterials did not show any catalytic activity in the MW-assisted oxidation of cyclohexane (not shown in the table for simplicity).

1@SWCNH-oxi exhibited the best catalytic performance: a maximum total (KA) yield of 29% was obtained after 1.5 h of MW irradiation at 50 °C (or 31% at 80 °C) in MeCN and in the presence of Hpca (Table 2). Although the heterogenization did not lead to a significant enhancement of the KA oil yield, it was revealed to be importantly advantageous for the separation and recyclability of the catalyst (see below).

Figure 7 shows the comparison of **1** supported on the different carbon materials for two MW irradiation temperatures (50 °C and 80 °C). The use of 80 °C does increase the yield of KA oil in all cases, up to a factor of about 2 for **1**@ND and

Table 2. Selected data[a] for the optimized MW-assisted oxidation of cyclohexane with TBHP catalyzed by [$FeCl_2$(Tpm)] (**1**) in MeCN and in the presence of Hpca.

Entry	Catalyst	Yield [%][b]			Total TOF[c] [h^{-1}]
		Cyclohexanol (A)	Cyclohexanone (K)	Total	
1	**1**@ND	4.6	2.3	6.9	46
2	**1**@NDox	7.3	5.0	12.3	95
3	**1**@NDoxNa	9.1	5.7	14.8	99
4	**1**@G-NPL	3.7	1.9	5.6	37
5	**1**@GO	8.7	5.3	14.0	93
6	**1**@rGO	1.9	0.9	2.8	19
7	**1**@SWCNH	8.9	5.3	14.2	82
8	**1**@SWCNH-oxi	16.9	11.9	28.8	192
9	**1**	19.7	7.4	27.1	181
10	–	0	0	0	–

[a] Reaction conditions: cyclohexane (5 mmol), catalyst (5 μmol, based on the iron complex **1**, 0.1 mol% vs. cyclohexane), TBHP (10 mmol), *n*(Hpca)/*n*(catalyst) = 40, 1.5 h under 20 W power MW irradiation, in acetonitrile (3 mL) at 50 °C. Amounts of cyclohexanone (K) and cyclohexanol (A) were determined by GC analysis after reduction of the aliquots with solid PPh_3[14] by using $MeNO_2$ as the standard. [b] Percentage molar yield ((mol of product)/(mol of cyclohexane)). [c] Total turnover frequency, defined as [(mol of A and K)/(mol of **1**)]/h.

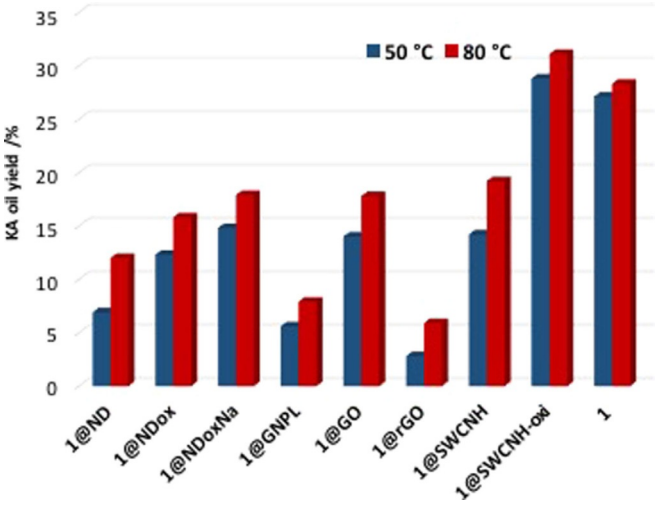

Figure 7. Effect of the temperature and type of nanostructured carbon material on the yield of KA oil obtained from oxidation of cyclohexane catalyzed by heterogenized **1**.

1@rGO (although these supports gave the worst results). The best results were obtained with the oxidized materials, showing the importance of surface oxygen groups as anchorage sites, as already reported in the literature.[4q,x,7b,15]

The effect of MW radiation on the catalytic performance of **1** in homogeneous conditions or supported on the different nanostructured materials was evaluated by comparison with the use of the conventional heating (oil bath) and is shown in Figure 8. For the same reaction conditions (including reaction time), the catalysts activity was always strongly enhanced by MW irradiation, while selectivity for the KA oil was preserved.

The stability of **1**@SWCNH-oxi was tested in terms of its recyclability up to nine consecutive cycles (see the Experimental Section) and is depicted in Figure 9. The catalyst activity and selectivity are maintained through a considerably high number of consecutive cycles: for example, after the fifth cycle, **1**@SWCNH-oxi still retains 90% of its initial activity. Moreover, the inductively coupled plasma (ICP) analysis of the corresponding supernatant phase revealed a leaching of **1** inferior to 1.1%.

However, after the ninth consecutive cycle, **1** is no longer supported on the carbon material, as confirmed by SEM energy-dispersive X-ray spectroscopy (EDS) analysis (Figure S2 in the Supporting Information).

Microwave-assisted oxidation of 1- or 2-phenylethanol

One of the best catalytic systems for the oxidation of cyclohexane, the scorpionate complex [$FeCl_2$(Tpm)] (**1**) supported on functionalized nanodiamonds (**1**@NDoxNa) was also tested for the solvent-free microwave-assisted oxidation of 1- and 2-phenylethanol according to Scheme 2.

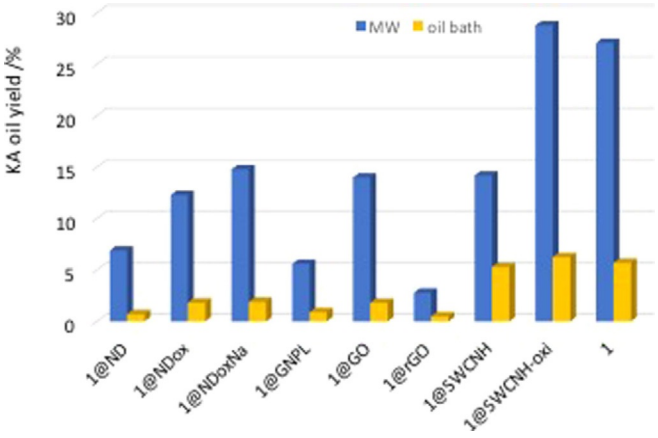

Figure 8. Effect of the heating mode (MW irradiation or oil bath) on the yield of KA oil obtained from oxidation of cyclohexane catalyzed by heterogenized **1** at 50 °C.

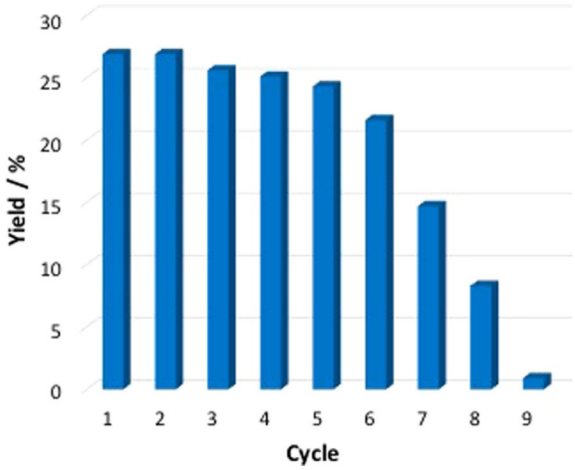

Figure 9. Effect of the number of catalytic cycles on the yield of KA oil obtained from oxidation of cyclohexane catalyzed by **1**@SWCNH-oxi.

Under the optimized conditions, 1 h of MW irradiation (25 W) at 80 °C, 97.1% yield of acetophenone and 96.9% yield of 2-phenylacetaldehyde were obtained from the selective MW-assisted oxidation of 1- and 2-phenylethanol in the presence of 0.1 mol% versus substrate of **1**@NDoxNa (turnover frequencies (TOFs) of 9.7×10^2 h^{-1}). No traces of byproducts were detected by GC-MS analysis in the final reaction mixtures for the above conditions. Moreover, control experiments in the absence of the catalyst led to 5% or 8% alcohol conversion, for 1-phenylethanol or 2-phenylethanol, respectively, highlighting the crucial role of **1** to efficiently catalyze the oxidation of the tested alcohols.

Catalyst recycling was tested for up to seven consecutive cycles for MW-assisted oxidation of 1-phenylethanol and it was found that the catalyst maintains almost the original level of activity after five reaction cycles: after the sixth cycle, **1**@NDoxNa still retains 90% of its initial activity (Figure 10).

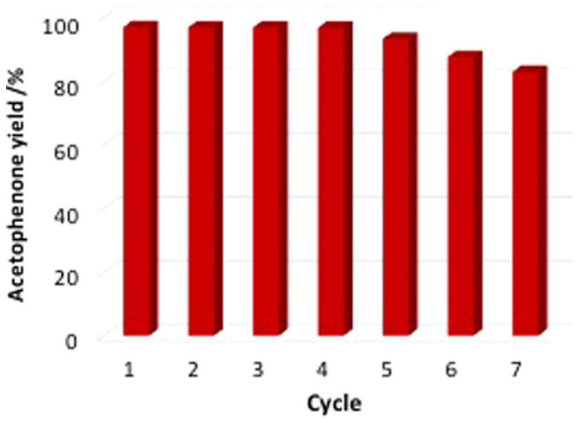

Figure 10. Effect of the number of catalytic cycles on the yield of acetophenone obtained from oxidation of 1-phenylethanol catalyzed by **1**@NDoxNa.

Conclusions

This work demonstrated that the C-scorpionate iron(II) catalyst $[FeCl_2(Tpm)]$ [Tpm = κ^3-$HC(C_3H_3N_2)_3$] (**1**), heterogenized on the SWCNH-oxi material leads to a highly selective, efficient, fast, and reusable catalytic system for the mild MW-assisted oxidation of cyclohexane. Moreover, **1**@NDoxNa exhibits good activity for the MW-induced solvent-free oxidation of both primary and secondary alcohols towards the formation of the corresponding aldehyde or ketone, respectively, a feature that is also noteworthy.

The best results were obtained with the oxidized materials, confirming the importance of surface oxygen groups as anchorage sites.

Experimental Section

Materials and instrumentation

All the reagents were purchased from commercial sources and used as received. Solvents were dried if necessary, by heating at reflux over the appropriate drying reagents and distilled under nitrogen prior to use. The $[FeCl_2(Tpm)]$ [Tpm = κ^3-$HC(C_3H_3N_2)_3$] complex was synthesized according to the protocol described in a previous work[4c] and characterized accordingly.

Scanning electron microscopy (SEM) and energy-dispersive X-ray spectroscopy (EDX) analyses were performed with a scanning electron microscope JEOL 7001F with Oxford light elements EDS detector and EBSD detector.

Reactions under microwave (MW) irradiation were performed in a focused Anton Paar Monowave 300 reactor fitted with a rotational system and an IR temperature detector, by using a 10 mL capacity cylindrical Pyrex tube with a 13 mm internal diameter.

Gas chromatographic (GC) measurements were performed by using a FISONS Instruments GC 8000 series gas chromatograph equipped with a FID detector and a capillary column (DB-WAX, column length: 30 m; column internal diameter: 0.32 mm) and run by the software Jasco-Borwin v.1.50. The temperature of injection was 240 °C. After the injection, the reaction temperature was maintained at either 100 °C (oxidation of cyclohexane) or 140 °C (oxidation of alcohols) for 1 min, then raised, by 10 °C min^{-1}, either to 180 °C (oxidation of cyclohexane) or 220 °C (oxidation of alcohols) and held at this temperature for 1 min. Helium was used as the carrier gas. GC-MS analyses were performed by using a PerkinElmer Clarus 600 C instrument (He as the carrier gas), equipped with two capillary columns (SGE BPX5; 30 m × 0.32 mm × 25 mm), one having an EI-MS (electron impact) detector and the other one with a FID detector. Reaction products were identified by comparison of their retention times with known reference compounds, and by comparing their mass spectra to fragmentation patterns obtained from the NIST spectral library stored in the computer software of the mass spectrometer.

Carbon material production and treatments

Graphene oxide (GO), reduced graphene oxide (rGO), and graphene nanoplatelets (G-NPL) were supplied from The Graphene Box (Spain). Single-walled carbon nanohorns (SWCNH) were supplied by Carbonium (Italy). Nanodiamonds (ND) were purchased from Sigma–Aldrich.

These carbon materials were used in their original forms, as purchased. For comparison with the pristine sample, SWCNH were oxidized in air, for 2 h at 400 °C (SWCNT-oxi). ND were oxidized with nitric acid (-ox); and oxidized with nitric acid with a subsequent treatment with NaOH (-ox-Na). The -ox material was obtained by treating the ND with a 5 M nitric acid solution (75 mL per gram of carbon material) for 3 h at reflux.[4q,x,7b,13] The solid was then filtered and washed with deionized water until a neutral pH value was obtained. The -ox-Na sample was achieved by subsequent treatment of the -ox material with a 20 mM NaOH aqueous solution (75 mL per gram of carbon material) for 1 h at reflux, followed by filtration and washing until neutral pH.[4q,x,7b,15]

Carbon material characterization

Samples were characterized by N_2 adsorption/desorption at −196 °C with a Quantachrome NOVA 4200e apparatus. The Brunauer–Emmett–Teller (BET) equation was applied to determine the apparent surface area.[16] X-ray photoelectron spectroscopy (XPS) analyses were performed with a VG Scientific ESCALAB 200A spectrometer using AlK_α radiation (1486.6 eV). The charge effect was corrected taking the C 1s peak as a reference (binding energy of 285 eV). CASAXPS software was used for data analysis.

Heterogenization protocol

The complexes were anchored onto the different carbon supports (0.15 g). The necessary amount to obtain ≈2% Fe per mass of carbon was weighed and dissolved in water (25 mL). Samples were left stirring at room temperature overnight, filtered, washed with water and methanol, and dried overnight at 40 °C in a vacuum oven. The Fe loading was confirmed by inductively coupled plasma (ICP) performed by Requimte Analytical Services of Nova University (Lisbon).

Catalytic activity tests

MW-assisted peroxidative oxidation of cyclohexane: Cyclohexane (0.54 mL, 5 mmol), catalyst immobilized onto a carbon material (1–10 μmol based on the iron complex; 0.02–0.2 mol% vs. cyclohexane), H_2O_2 (30% aq. sol., 10 mmol) or TBHP (70% aq. sol., 10 mmol), and MeCN (3 mL) were placed in the cylindrical Pyrex tube of the microwave reactor. Optionally, an additive ($n_{additive}/n_{catalyst}=40$) was added. The reaction vessel was closed and the contents were stirred and irradiated (up to 20 W) for 0.25–24 h at 50–80 °C. CAUTION: if using hydrogen peroxide, the combination of air or molecular oxygen and H_2O_2 with organic compounds at elevated temperatures may be explosive! After the reaction, the mixture was cooled to room temperature and the suspension (owing to the supported catalyst) was centrifuged and filtered to prepare the samples for GC analysis. Cycloheptanone or nitromethane (internal standard) and diethyl ether (to extract the substrate and the organic products from the reaction mixture) were added to the filtrate. The obtained mixture was stirred for 10 min and then a sample (1 μL) was taken from the organic phase and analyzed by gas chromatography using Shul'pin's method.[14,17] This method allows us the estimate of concentrations of formed cyclohexyl hydroperoxide, cyclohexanol, and cyclohexanone. Attribution of peaks was made by comparison with chromatograms of authentic samples. For precise determination of the product concentrations, only data obtained after the reduction of the reaction sample with PPh_3 were typically used, taking into account that the original reaction mixture contained the three products: cyclohexyl hydroperoxide (as the primary product), cyclohexanol, and cyclohexanone.

For comparison, cyclohexane oxidation reactions were performed in round-bottom flasks under the same reaction conditions but by using an oil bath as the heating source (up to 3 mL total volume).

Blank tests were performed in iron-free systems, but in the presence of the nanostructured carbon materials.

Recyclability of the catalyst with the highest catalytic activity was investigated, for up to nine cycles. Each run was initiated after the preceding one, upon addition of new typical portions of all other reagents. After completion of each run, the products were analyzed as above-mentioned and the catalyst was recovered by filtration, thoroughly washed with acetonitrile, and dried overnight in an oven at 80 °C.

MW-assisted oxidation of alcohols: TBHP (70% aq. sol., 10 mmol) was added to 1- or 2-phenylethanol (5 mmol) and the catalyst (1–10 μmol based on the iron complex; 0.02–0.2 mol% vs. substrate) suspension. The reaction vessel was closed and the contents were stirred and irradiated (up to 20 W) for 0.5–24 h at 80 °C. Then, the mixture was cooled to room temperature, the internal standard (150 μL of benzaldehyde or cyclopentanone, respectively, for the secondary or primary alcohol) and diethyl ether (5 mL, to extract the substrate and the organic products from the reaction medium) were added and the mixture was stirred for 10 min. A sample (1 μL) was taken from the organic phase and analyzed by GC (or GC-MS) by using the internal standard method.

Blank tests were performed in an iron-free system, but in the presence of the nanostructured carbon materials for the different substrates.

Recyclability of the catalyst with the highest catalytic activity was investigated, for up to seven cycles. Each run was initiated after the preceding one upon addition of new typical portions of all other reagents. After completion of each run, the products were analyzed as above-mentioned and the catalyst was recovered by filtration, thoroughly washed with methanol, and dried overnight in an oven at 80 °C.

Acknowledgments

We are grateful for the financial support received from the Fundação para a Ciência e a Tecnologia (FCT), Portugal, and its projects UID/QUI/00100/2013, PTDC/QEQ-ERQ/1648/2014, and PTDC/QEQ-QIN/3967/2014. This work is a result of project "AIProcMat@N2020—Advanced Industrial Processes and Materials for a Sustainable Northern Region of Portugal 2020", with the reference NORTE-01-0145-FEDER-000006, supported by Norte Portugal Regional Operational Programme (NORTE 2020), under the Portugal 2020 Partnership Agreement, through the European Regional Development Fund (ERDF), and of Project POCI-01-0145-FEDER-006984-Associate Laboratory LSRE-LCM funded by ERDF through COMPETE2020-POCI—and by national funds through FCT. S.A.C.C. acknowledges the Investigador FCT program (IF/01381/2013/CP1160/CT0007), with financing from the European Social Fund and the Human Potential Operational Program.

Conflict of interest

The authors declare no conflict of interest.

Keywords: microwave-assisted reactions · nanostructured carbon support · oxidation · recyclable · scorpionate iron catalyst

[1] a) *Ullmann's Encyclopedia of Industrial Chemistry, 6th ed.*, Wiley-VCH, Weinheim, **2002**; b) Metal Catalysis *in Industrial Organic Processes* (Eds.: G. P. Chiusoli, P. M. Maitlis), Royal Society of Chemistry, Cambridge, **2006**.

[2] a) L. M. D. R. S. Martins, A. J. L. Pombeiro, *Coord. Chem. Rev.* **2014**, *265*, 74–88; b) L. M. D. R. S. Martins, A. J. L. Pombeiro in *Advances in Organometallic Chemistry and Catalysis, The Silver/Gold Jubilee ICOMC Celebratory Book* (Ed.: A. J. L. Pombeiro), Wiley, Hoboken, NJ, **2013**, pp. 285–294; c) L. M. D. R. S. Martins, A. J. L. Pombeiro, *Eur. J. Inorg. Chem.* **2016**, 2236–2252.

[3] A. P. C. Ribeiro, L. M. D. R. S. Martins, A. J. L. Pombeiro, *Green Chem.* **2017**, *19*, 1499–1501.

[4] a) A. I. F. Venâncio, L. M. D. R. S. Martins, J. da Silva, A. J. L. Pombeiro, *Inorg. Chem. Commun.* **2003**, *6*, 94–96; b) A. I. F. Venâncio, M. da Silva, L. M. D. R. S. Martins, J. da Silva, A. J. L. Pombeiro, *Organometallics* **2005**, *24*, 4654–4665; c) T. F. S. Silva, E. Alegria, L. M. D. R. S. Martins, A. J. L. Pombeiro, *Adv. Synth. Catal.* **2008**, *350*, 706–716; d) A. Karmakar, L. M. D. R. S. Martins, S. Hazra, M. F. C. G. Silva, A. J. L. Pombeiro, *Cryst. Growth Des.* **2016**, *16*, 1837–1849; e) S. Enthaler, K. Junge, M. Beller,

Angew. Chem. Int. Ed. **2008**, *47*, 3317 – 3321; *Angew. Chem.* **2008**, *120*, 3363 – 3367; f) R. H. Morris, *Chem. Soc. Rev.* **2009**, *38*, 2282 – 2291; g) M. N. Kopylovich, K. T. Mahmudov, M. F. C. G. Silva, L. M. D. R. S. Martins, M. L. Kuznetsov, T. F. S. Silva, J. J. R. Fraústo da Silva, A. J. L. Pombeiro, *Phys. Org. Chem.* **2011**, *24*, 764 – 773; h) R. R. Fernandes, J. Lasri, M. da Silva, J. A. L. Silva, J. Silva, A. J. L. Pombeiro, *J. Mol. Catal. A* **2011**, *351*, 100 – 111; i) R. R. Fernandes, J. Lasri, M. da Silva, J. A. L. Silva, J. Silva, A. J. L. Pombeiro, *Appl. Catal. A* **2011**, *402*, 110 – 120; j) M. Alexandru, M. Cazacu, A. Arvinte, S. Shova, C. Turta, B. C. Simionescu, A. Dobrov, E. C. B. A. Alegria, L. M. D. R. S. Martins, A. J. L. Pombeiro, V. B. Arion, *Eur. J. Inorg. Chem.* **2014**, 120 – 131; k) T. F. S. Silva, M. F. G. Silva, G. S. Mishra, L. M. D. R. S. Martins, A. J. L. Pombeiro, *J. Organomet. Chem.* **2011**, *696*, 1310 – 1318; l) M. N. Kopylovich, T. C. O. MacLeod, M. Haukka, G. I. Amanullayeva, K. T. Mahmudov, A. J. L. Pombeiro, *J. Inorg. Biochem.* **2012**, *115*, 72 – 77; m) D. S. Nesterov, E. N. Chygorin, V. N. Kokozay, V. V. Bon, R. Boca, Y. N. Kozlov, L. S. Shul'pina, J. Jezierska, A. Ozarowski, A. J. L. Pombeiro, G. B. Shul'pin, *Inorg. Chem.* **2012**, *51*, 9110 – 9122; n) M. J. Ingleson, R. A. Layfield, *Chem. Commun.* **2012**, *48*, 3579 – 3589; o) E. E. Karslyan, L. S. Shul'pina, Y. N. Kozlov, A. J. L. Pombeiro, G. B. Shul'pin, *Catal. Today* **2013**, *218*, 93 – 98; p) K. T. Mahmudov, M. N. Kopylovich, M. Haukka, G. S. Mahmudova, E. F. Esmaeila, F. M. Chyragov, A. J. L. Pombeiro, *J. Mol. Struct.* **2013**, *1048*, 108 – 112; q) L. M. D. R. S. Martins, M. P. de Almeida, S. A. C. Carabineiro, J. L. Figueiredo, A. J. L. Pombeiro, *ChemCatChem* **2013**, *5*, 3847 – 3856; r) L. M. D. R. S. Martins, A. Martins, E. Alegria, A. P. Carvalho, A. J. L. Pombeiro, *Appl. Catal. A* **2013**, *464*, 43 – 50; s) M. Sutradhar, M. Silva, A. J. L. Pombeiro, *Inorg. Chem. Commun.* **2013**, *30*, 42 – 45; t) M. N. M. Milunovic, L. M. D. R. S. Martins, E. Alegria, A. J. L. Pombeiro, R. Krachler, G. Trettenhahn, C. Turta, S. Shova, V. B. Arion, *Dalton Trans.* **2013**, *42*, 14388 – 14401; u) G. B. Shul'pin, M. V. Kirillova, L. S. Shul'pina, A. J. L. Pombeiro, E. E. Karslyan, Y. N. Kozlov, *Catal. Commun.* **2013**, *31*, 32 – 36; v) A. Karmakar, L. M. D. R. S. Martins, M. da Silva, S. Hazra, A. J. L. Pombeiro, *Catal. Lett.* **2015**, *145*, 2066 – 2076; w) D. S. Nesterov, O. V. Nesterova, M. Silva, A. J. L. Pombeiro, *Catal. Sci. Technol.* **2015**, *5*, 1801 – 1812; x) L. M. D. R. S. Martins, A. P. C. Ribeiro, S. A. C. Carabineiro, J. L. Figueiredo, A. J. L. Pombeiro, *Dalton Trans.* **2016**, *45*, 6816 – 6819; y) N. M. R. Martins, K. T. Mahmudov, M. da Silva, L. M. D. R. S. Martins, A. J. L. Pombeiro, *New J. Chem.* **2016**, *40*, 10071 – 10083; z) M. Sutradhar, E. Alegria, K. T. Mahmudov, M. da Silva, A. J. L. Pombeiro, *RSC Adv.* **2016**, *6*, 8079 – 8088; aa) M. Mendes, A. P. C. Ribeiro, E. Alegria, L. M. D. R. S. Martins, A. J. L. Pombeiro, *Polyhedron* **2017**, *125*, 151 – 155; ab) A. P. C. Ribeiro, L. M. D. R. S. Martins, A. J. L. Pombeiro, *Green Chem.* **2017**, *19*, 4811 – 4815; ac) A. P. C. Ribeiro, L. M. D. R. S. Martins, E. Alegria, I. A. S. Matias, T. A. G. Duarte, A. J. L. Pombeiro, *Catalysts* **2017**, *7*, 230.

[5] a) J. P. Lellouche, M. Piran, L. Shahar, J. Grinblat, C. Pirlot, *J. Mater. Chem.* **2008**, *18*, 1093 – 1099; b) S. A. Mamuru, K. I. Ozoemena, T. Fukuda, N. Kobayashi, T. Nyokong, *Electrochim. Acta* **2010**, *55*, 6367 – 6375; c) L. Saghatforoush, M. Hasanzadeh, N. Shadjou, B. Khalilzadeh, *Electrochim. Acta* **2011**, *56*, 1051 – 1061; d) H. L. Liu, Y. Y. Cui, P. Li, Y. M. Zhou, X. S. Zhu, Y. W. Tang, Y. Chen, T. H. Lu, *Analyst* **2013**, *138*, 2647 – 2653; e) M. E. Lipinska, S. L. H. Rebelo, C. Freire, *J. Mater. Sci.* **2014**, *49*, 1494 – 1505; f) A. Rezaeifard, M. Jafarpour, *Catal. Sci. Technol.* **2014**, *4*, 1960 – 1969; g) L. P. Zhang, W. J. Zhang, P. Serp, W. H. Sun, J. Durand, *ChemCatChem* **2014**, *6*, 1310 – 1316; h) O. O. Fashedemi, K. I. Ozoemena, *RSC Adv.* **2015**, *5*, 22869 – 22878; i) N. Kuznik, M. M. Tomczyk, M. Wyskocka, L. Przypis, A. P. Herman, R. Jedrysiak, K. K. Koziol, S. Boncel, *Int. J. Nanomed.* **2015**, *10*, 3581 – 3591; j) S. Rayati, Z. Sheybanifard, *J. Porphyrins Phthalocyanines* **2015**, *19*, 622 – 630.

[6] a) Y. Dong, J. Li, L. Shi, J. Xu, X. B. Wang, Z. G. Guo, W. M. Liu, *J. Mater. Chem. A* **2013**, *1*, 644 – 650; b) Z. F. Li, S. J. Wu, H. Ding, H. M. Lu, J. Y. Liu, Q. S. Huo, J. Q. Guan, Q. B. Kan, *New J. Chem.* **2013**, *37*, 4220 – 4229; c) P. Kumar, G. Singh, D. Tripathi, S. L. Jain, *RSC Adv.* **2014**, *4*, 50331 – 50337; d) Z. F. Li, S. J. Wu, D. F. Zheng, H. Ding, X. F. Wang, X. Y. Yang, Q. S. Huo, J. Q. Guan, Q. B. Kan, *ChemPlusChem* **2014**, *79*, 716 – 724; e) H. L. Su, Z. F. Li, Q. S. Huo, J. Q. Guan, Q. B. Kan, *RSC Adv.* **2014**, *4*, 9990 – 9996; f) X. Zhou, T. Zhang, C. W. Abney, Z. Li, W. B. Lin, *ACS Appl. Mater. Interfaces* **2014**, *6*, 18475 – 18479; g) H. L. Su, S. J. Wu, Z. F. Li, Q. S. Huo, J. Q. Guan, Q. B. Kan, *Appl. Organomet. Chem.* **2015**, *29*, 462 – 467; h) G. E. Yuan, G. Q. Zhang, Y. F. Zhou, F. L. Yang, *RSC Adv.* **2015**, *5*, 26132 – 26140.

[7] a) L. Zhao, A. Shiino, H. M. Qin, T. Kimura, N. Komatsu, *J. Nanosci. Nanotechnol.* **2015**, *15*, 1076 – 1082; b) M. Sutradhar, L. M. D. R. S. Martins, S. A. C. Carabineiro, M. F. C. Guedes da Silva, J. G. Buijnsters, J. L. Figueiredo, A. J. L. Pombeiro, *ChemCatChem* **2016**, *8*, 2254 – 2266.

[8] a) X. Gao, J. Jang, S. Nagase, *J. Phys. Chem. C* **2010**, *114*, 832 – 842; b) L. M. Pastrana-Martínez, S. Morales-Torres, V. Likodimos, P. Falaras, J. L. Figueiredo, J. L. Faria, A. M. T. Silva, *Appl. Catal. B* **2014**, *158 – 159*, 329 – 340.

[9] L. M. D. R. S. Martins, S. A. C. Carabineiro, J. Wang, B. G. M. Rocha, F. J. Maldonado-Hódar, A. J. L. Pombeiro, *ChemCatChem* **2017**, *9*, 1211 – 1221.

[10] a) M. N. Kopylovich, A. P. C. Ribeiro, E. C. B. A. Alegria, N. M. R. Martins, L. M. D. R. S. Martins, A. J. L. Pombeiro, *Adv. Organomet. Chem.* **2015**, *63*, 91 – 174; b) A. Sabbatini, L. M. D. R. S. Martins, K. T. Mahmudov, M. N. Kopylovich, M. G. B. Drew, C. Pettinari, A. J. L. Pombeiro, *Catal. Commun.* **2014**, *48*, 69 – 72; c) A. J. L. Pombeiro, L. M. D. R. S. Martins, A. P. C. Ribeiro, S. A. C. Carabineiro, J. L. Figueiredo (Instituto Superior Técnico, Instituto Superior De Engenharia De Lisboa, Universidade Do Porto, Portugal), Portuguese patent request PT109062, **2015**, request for international extension to other countries PCT/PT2016/000019, **2016**, and world wide patent application WO2017116253A1, **2017**; d) J. Wang, L. M. D. R. S. Martins, A. P. C. Ribeiro, S. A. C. Carabineiro, J. L. Figueiredo, A. J. L. Pombeiro, *Chem. Asian J.* **2017**, *12*, 1915 – 1919; e) N. M. R. Martins, L. M. D. R. S. Martins, C. O. Amorim, V. S. Amaral, A. J. L. Pombeiro, *Catalysts* **2017**, *7*, 222 – 239.

[11] A. B. Deshmukh, M. V. Shelke, *RSC Adv.* **2013**, *3*, 21390 – 21393.

[12] a) S. Park, J. An, I. Jung, R. D. Piner, S. J. An, X. Li, A. Velamakanni, R. S. Ruoff, *Nano Lett.* **2009**, *9*, 1593 – 1597; b) H. P. Cong, X. C. Ren, P. Wang, S. H. Yu, *Energ. Environ. Sci.* **2013**, *6*, 1185 – 1191; c) Z. Ling, C. Yu, X. Fan, S. Liu, J. Yang, M. Zhang, G. Wang, N. Xiao, J. Qiu, *Nanotechnology* **2015**, *26*, 374003; d) J. L. Figueiredo, *J. Mater. Chem. A*, **2013**, *1*, 9351 – 9364.

[13] a) J. L. Figueiredo, M. F. R. Pereira, M. M. A. Freitas, J. J. M. Órfão, *Carbon* **1999**, *37*, 1379 – 1389; b) J. L. Figueiredo, M. F. R. Pereira, M. M. A. Freitas, J. J. M. Órfão, *Ind. Eng. Chem. Res.* **2007**, *46*, 4110 – 4115; c) S. A. C. Carabineiro, M. F. R. Pereira, J. J. M. Órfão, J. L. Figueiredo in *Activated Carbon: Classifications, Properties and Applications* (Ed.: J. F. Kwiatkowski), Nova Science Pub Inc., New York, **2011**, pp. 125 – 168.

[14] a) G. B. Shul'pin, G. V. Nizova, *React. Kinet. Catal. Lett.* **1992**, *48*, 333 – 338; b) G. B. Shul'pin, M. G. Matthes, V. B. Romakh, M. I. F. Barbosa, J. L. T. Aoyagi, D. Mandelli, *Tetrahedron* **2008**, *64*, 2143 – 2152; c) G. B. Shul'pin, *Mini-Rev. Org. Chem.* **2009**, *6*, 95 – 104; d) G. B. Shul'pin, *Org. Biomol. Chem.* **2010**, *8*, 4217 – 4228; e) G. B. Shul'pin, *Dalton Trans.* **2013**, *42*, 12794 – 12818.

[15] a) N. Mahata, A. R. Silva, M. F. R. Pereira, C. Freire, B. de Castro, J. L. Figueiredo, *J. Colloid Interface Sci.* **2007**, *311*, 152 – 158; b) F. Maia, N. Mahata, B. Jarrais, A. R. Silva, M. F. R. Pereira, C. Freire, J. L. Figueiredo, *J. Mol. Catal. A* **2009**, *305*, 135 – 141.

[16] S. Brunauer, P. H. Emmett, E. Teller, *J. Am. Chem. Soc.* **1938**, *60*, 309 – 319.

[17] G. B. Shul'pin in *Transition Metals for Organic Synthesis, Vol. 2, 2nd ed.* (Eds.: M. Beller, C. Bolm), Wiley-VCH, Weinheim, **2004**.

Manuscript received: December 23, 2017
Revised manuscript received: January 16, 2018
Accepted manuscript online: January 22, 2018
Version of record online: March 8, 2018